Mie scattering from a sonoluminescing air bubble in water

W. J. Lentz, Anthony A. Atchley, and D. Felipe Gaitan

A single bubble of air in water can emit pulses of blue-white light that have durations of less than 50 ps while it is oscillating in an acoustic standing wave. The emission is called sonoluminescence. A knowledge of the bubble diameter throughout the cycle, and in particular near the time of sonoluminescence emission, can provide important information about the phenomenon. A new Mie scattering technique is developed to determine the size of the bubble through its expansion and collapse during the acoustic cycle. The technique does not rely on an independent means of calibration or on accurate measurements of the scattered intensity.

Key words: Sonoluminescence, Mie theory, scattering, bubble, sizing.

1. Introduction

A single, stable gas bubble can be trapped in a liquid, through a process known as acoustic levitation, by an acoustic-standing-wave field setup in that liquid.[1] Once levitated, a bubble can be held in place for hours. In response to the levitation field, the bubble can be made to undergo radial (volume) or shape oscillations of varying amplitude by proper choice of standing-wave amplitude and frequency. Gaitan *et al.*[1] showed that within a narrow range of these drive parameters the bubble undergoes large-amplitude, apparently radially symmetric oscillations. The diameter of the bubble might range from a maximum of approximately 100 μm during the expansion phase of the oscillation down to a minimum diameter of less than 10 μm. At the end of the collapse phase of its oscillation cycle, the bubble emits a short burst of blue-white light called sonoluminescence (SL).

SL displays several remarkable features. Whereas the driving field typically has a period of tens of microseconds, the duration of the SL pulse is less than 50 ps.[2,3] The pulse spectrum is broadband and increases in intensity into the ultraviolet.[4,5] Single SL pulses are isotropic and unpolarized. The SL amplitude and periodicity can be extremely stable-. Although several mechanisms have been proposed to account for this phenomenon, there is still no fully satisfactory explanation.[6–8] Because SL is intimately linked to the dynamics of the bubble, it is important to understand the behavior of the bubble during its expansion and collapse over one acoustic cycle. It is particularly important to know the diameter and the velocity of the bubble near the time of emission.

The purpose of this paper is to explain a new laser-scattering technique for sizing the bubble, and to measure the diameter of the sonoluminescing bubble. Previous papers[1,5] have relied on the scattered intensity of laser light and on an independent calibration. In one case calibration measurements were made at known bubble sizes,[1] and in the other[5] a hydrodynamic calculation was made. We use a different technique. Based on Mie scattering theory,[9–11] our technique relies on neither an independent calibration of the size of the scatterer nor accurate measurements of the absolute intensity of scattered light. It allows one to measure the diameter and the rate of change of diameter of the bubble near the time of luminescence.

Aside from a chance to learn about SL, laser scattering from oscillating bubbles presents a somewhat different side of Mie scattering. The fundamental parameter is the size parameter $\alpha = \pi d/\lambda$, where d is the diameter of the scatterer and λ is the wavelength of the incident light in the surrounding medium. In SL applications d changes continuously by over a factor of 10, and the intensity of the scattered light changes by approximately a factor of 100 during the 30-μs acoustic cycle. This is in contrast to scattering from a solid sphere, in which the wavelength might be changed by a relatively

The authors are with Naval Postgraduate School, Code PHLZ, 833 Dyer Road, Monterey, California 93943.

Received 28 February 1994; revised manuscript received 17 August 1994.

0003-6935/95/152648-07$06.00/0.

small amount. The angular scattering pattern for a bubble is also different from that of a solid sphere.

2. Method

Two concepts form the basis of the method used to size sonoluminescing bubbles. The concepts are (1) how the scattered intensity depends on the diameter of the scatterer d for a fixed solid angle and (2) how the scattered intensity depends on angle for a fixed diameter.

Figure 1 shows the calculated intensity of scattered light at a fixed angle of 47° (from forward) as a function of diameter. The dark curve in Fig. 1 is a weighted average of five angles in 1° degree increments centered around 47° with a 10-point smoothing. The weighting is chosen to match the experimental viewing angle, and the smoothing is necessary because of the signal averaging and the broad laser-diode emission. The indices of refraction of the air inside the bubble and the water surrounding the bubble are assumed to be 1.00 and 1.33, respectively. The wavelength of the laser light is 693 nm.

The broad peaks are actually clusters of narrow peaks or lobes that are characteristic of Mie scattering and are called lobe clusters (LC's). The narrow peaks have been averaged together by the finite field of view. Figure 1 shows that the scattered intensity is a multivalued function of diameter. The implication is that a measurement of the scattered intensity is not sufficient to size the scatterer uniquely. Averaging over more angles does not completely solve the problem, especially at small diameters. An independent means of calibration is necessary before sizing is possible. Background subtraction and detector linearity must also be taken into consideration when one is sizing scatterers from measurements of the absolute intensity of scattered light.

The light curve in Fig. 1 represents the (5° weighted average, smoothed) scattered intensity for an angle centered at 53°, along with the 47° (dark) curve. It can be seen that the maxima and the minima of the LC have shifted relative to the dark curve. In fact the pattern shifts in the direction of larger diameter for larger scattering angles. Also, notice that two maxima nearly coincide at a diameter of approximately 52 μm. It is important to point out that this is the only value of diameter (in our range of interest) where two maxima coincide.

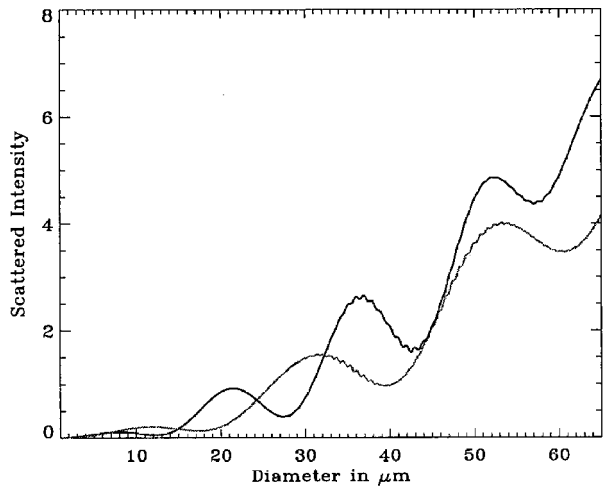

Fig. 1. Simultaneous LC scattering at scattering angles of 47° (dark curve) and 53° (light curve).

As the bubble responds to the acoustic field, its diameter changes with time. Suppose that one were to examine the scattered intensity as a function of time during the expansion phase of the bubble's motion. In this case one would observe that the scattered intensity generally increased, with modulations that were due to the LC, as the diameter increased. The detector output would roughly mimic one of the curves in Fig. 1 as one moves from left to right (in the direction of increasing diameter) as time increased. During the collapse phase, the detector output would decrease as one moves from right to left in Fig. 1.

To appreciate the foundation of the technique, imagine that two identical detectors were used to observe the scattering. If the detectors were located at the same scattering angle, the outputs of the detectors as functions of time would be identical, reaching maxima and minima at the same time. If one detector were moved to a different angle, its output would shift relative to that of the stationary detector, just as the two curves in Fig. 1 are shifted relative to each other. By varying the angle of the adjustable detector, it is possible to shift the pattern until two initially different peaks coincide in time. If the scattering angles were those from Fig. 1, the coincident peaks would overlap in time when the bubble diameter was approximately 52 μm. Aside from yielding the value of diameter at a particular time, finding coincident peaks yields one other piece of information. Because it occurs at a unique value of diameter, the coincidence identifies the peaks so that they are distinguishable from the others observed at the same angle. That is, the coincidence identifies which of the several peaks present in Fig. 1 is known without reliance on a measure of the absolute scattered intensity or an independent means of calibration!

Once a particular peak is identified, there are two ways to determine the diameter of the bubble at other times. One can measure the time of occurrence of the other unique features of the scattered signal, such as maxima and minima, detected at the same angle. The corresponding diameters are found when the measured features are matched to the predicted ones. Alternatively, one can change the angle of the detector, keeping track of the identified peak or minima. In practice the minima are flatter and have poorer signal-to-noise ratios than the peaks, and because peaks provide continuous sizing with angle, the minima were not used. To illustrate the matching, a graph of diameter versus peak number has been constructed for a family of scattering angles, as shown in Fig. 2. For a fixed viewing angle, one

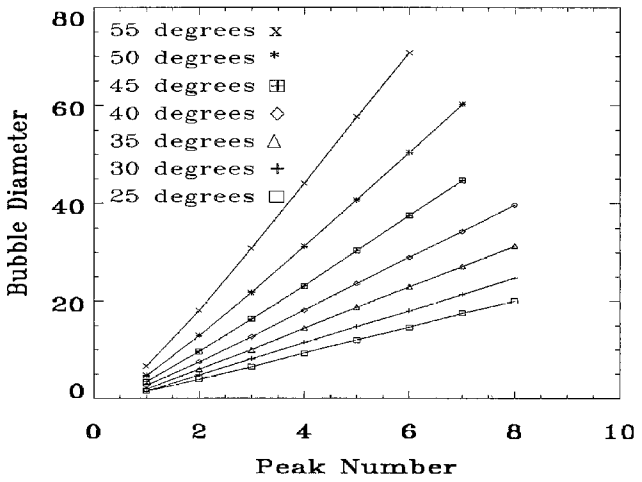

Fig. 2. Bubble diameter versus LC peak number for various scattering angles.

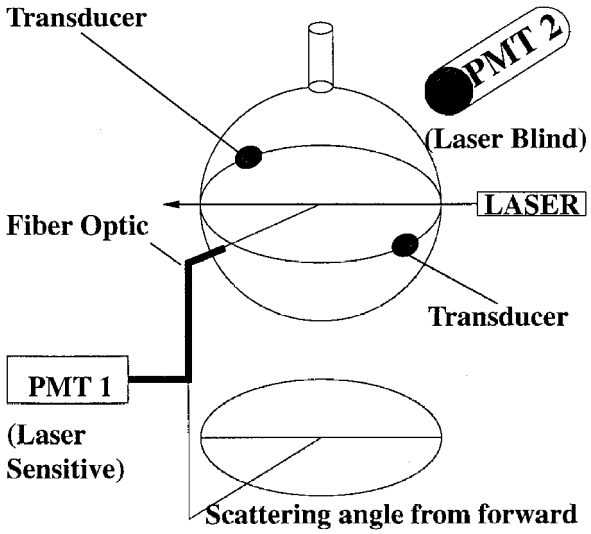

Fig. 3. Experimental setup, with a pulsed 693-nm laser. PMT 1, Hamamatsu R928p; PMT 2, RCA 5819 PMT.

moves along the appropriate diagonal line, picking out diameters at peak numbers. For a given peak, changing the scattering angle changes the corresponding diameter on a vertical line.

This technique is independent of the absolute intensity of the scattered signal. Techniques that rely on measurements of the absolute scattered intensity must struggle with questions of detector linearity, rise and fall times, background subtraction, calibration, multivalued scattering, and other complicating factors. Our technique avoids these questions altogether. It does, however, rely on the repeatability of the bubble's motion, and it assumes that the bubble maintains its spherical shape and that the indices of refraction of the air and the water remain constant during the cycle. These assumptions are discussed further below.

3. Experimental Apparatus

SL is emitted by a single air bubble that is levitated in an acoustic standing wave generated in a water-filled, 100-mL spherical flask. The water is distilled and degassed. The standing wave is excited by means of two hollow, cylindrical, piezoelectric transducers cemented to the outside of the flask. The transducers are driven at approximately 26 kHz to a few volts amplitude with a function generator, through an inductive impedance-matching circuit. The drive frequency is adjusted to set up a radially symmetric standing wave in the flask. A small amount of air is injected into the flask with a hypodermic syringe. A portion of the injected air evolves into a single bubble levitated at the acoustic pressure antinode located at the center of the flask. With proper adjustment of the drive amplitude and frequency, this bubble reaches a state in which it undergoes cyclic, large-amplitude, radial oscillations, while it emits one pulse of SL per acoustic cycle.

The experimental setup is shown in Fig. 3. The laser was a Toshiba TOLD9140 laser diode that emitted 20 mW of 693-nm radiation into a 1-mm beam with pulse as well as continuous capability. Two photomultiplier tubes (PMT's) were used. An RCA 5819 PMT, which is substantially insensitive to the laser light, was used to detect the SL directly. The second PMT, a Hamamatsu extended red R928p, detects the scattered laser light, which is collected with a fiber-optic bundle. The entrance end of the fiber bundle was rotated around the bubble from the 5° laser beam stop to nearly 180° from forward with ±0.25° accuracy. The field view of the fiber bundle was 5°. A lens could also be attached to the fiber bundle to increase the field of view to approximately 22°.

A. Sizing by the Use of Measurements of Scattered Intensity

An example of the scattering from a sonoluminescing bubble is shown in Fig. 4. The top trace shows the output of the PMT that was used to monitor the SL. The bottom trace shows the laser scattering. A

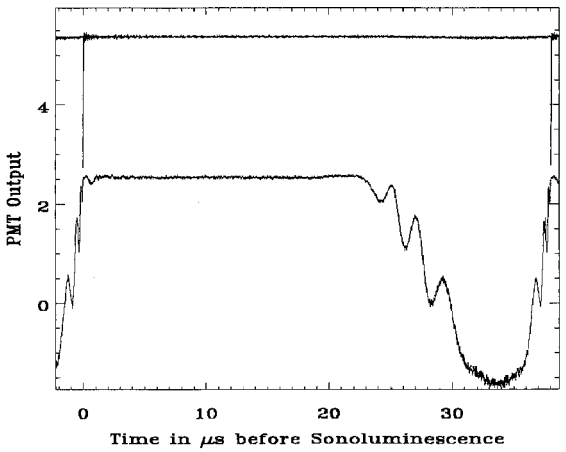

Fig. 4. SL and Mie scattering with an LC graph, showing the output of two PMT's as a function of time. The upper trace is the output of the PMT used to monitor SL. The lower trace is the output of the PMT used to detect the laser scattering.

negative-going PMT signal indicates increasing scattered intensity. The PMT was overloaded at the peak of the laser scattering. The SL occurs at the apparent minimum of the bubble collapse. It is worthwhile to mention that the shape of the curve in Fig. 4 can be changed just by changing the collection angle, because Mie scattering is not isotropic. That is, any number of different curves can be measured for the same bubble motion. The scattering in Fig. 5 (extended scattering) lacks LC's because the fiber bundle was fitted with a lens that collected a 22° field of view at a scattering angle of 45°. The shape of the scattering agrees with previous measurements.[5]

The main purpose of Fig. 5 is to illustrate some difficulties associated with sizing from measurements of absolute scattered intensity. The foremost is that it is difficult to measure the scattered laser light accurately. The background light that is scattered from the flask and the host liquid must be subtracted from the scattering from the bubble. The bubble center may move in the laser beam during the cycle, which causes a change in scattering. The rapidly changing intensity of the scattered light must be linearly measured for over 2 decades in the presence of the background. A calibration must be performed under the same conditions. At the most interesting time, when the bubble luminesces, the bubble scattering and the background light have the poorest signal-to-noise ratio. Also, the signal is rapidly decreasing just before SL, and both PMT's and semiconductor detectors have a worse response to decreasing signals than to increasing signals. In addition to the experimental problems, there may be difficulties in finding a calibration point to calibrate the intensity measurements. The calibration may change as the bubble compresses and changes the internal index of refraction.

B. Mie Sizing by Lobe Clusters

The solid angle in which the signal was collected in Fig. 5 was large enough to average out most of the LC's present in Fig. 4. The result is a scattered intensity that is roughly proportional to the diameter squared. Our technique relies on the presence of LC's, obtained with smaller viewing angles. For a smaller viewing angle of 5°, the diameter-squared increase in scattered intensity is modulated by LC structure.

The relationship between peak number and diameter in Fig. 2 is approximately linear, but the slope depends on scattering angle. The diameter that corresponds to a given LC increases continuously as the scattering angle is increased. This means that a given LC will slide toward larger sizes as the scattering angle is increased. It should be pointed out that there is a first LC peak (counting from zero diameter). The first LC peak for 25° occurs at a diameter of approximately 1.5 μm. Once any one LC is identified, the size of the bubble can be determined at every LC. Because the peaks move to larger sizes with larger angles, a continuous sizing can be made by variation of the scattering angle.

The usefulness of the technique is demonstrated by measurement of the diameter of a bubble near the time of SL emission. The average amount of scattered light that enters the PMT was reduced by pulsing the laser for approximately 4 μs near the time of SL. This permitted the PMT gain to be increased for the smaller bubble diameters without damaging the PMT. The top trace in Fig. 6 shows the output of the PMT that was used to monitor the SL. This trace shows a burst of noise as the laser pulses on. All sizing is done relative to the negative SL spike taken as zero time. The bottom trace shows the scattered laser light. The beginning of the laser pulse is evident, as well as the smooth modulations that are due to LC.

The calculated scattered intensity as a function of diameter is shown in Fig. 7(a) for scattering angles of 45° (dark curve) and 48° (light curve). The horizontal axis for the calculations has been reversed so that bubble diameter decreases to the right of the figure. The corresponding measured scattered signals are shown in Fig. 7(b). The signals are all inverted for

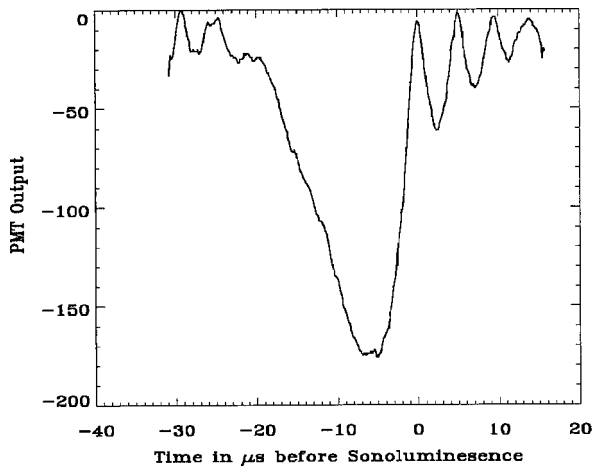

Fig. 5. 22° field-of-view scattering.

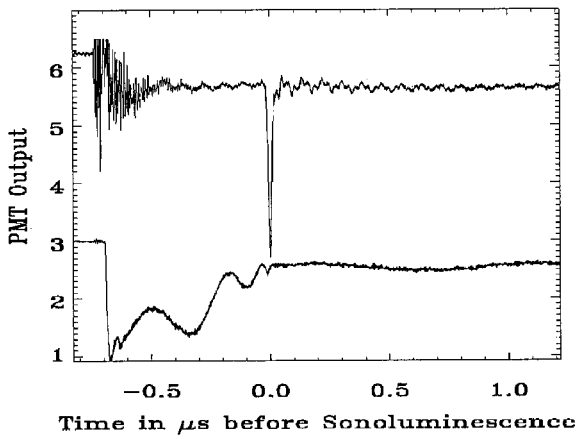

Fig. 6. SL and pulsed laser-scattering graph, showing the outputs of the PMT's used to monitor SL (upper trace) and scattering (lower trace) as functions of time. The laser pulse starts at −0.7 ms. The modulation in the scattered intensity corresponds to LC.

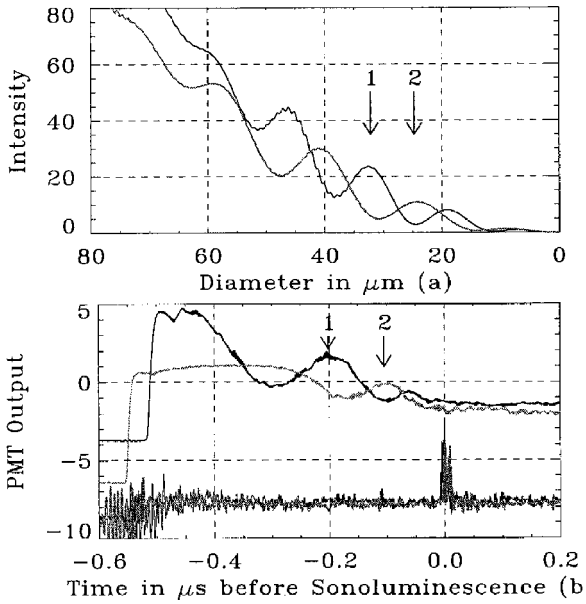

Fig. 7. LC identification by comparison of (a) theoretical and (b) experimental scattering at 45° (dark curve) and 48° (light curve). 1, scattering at −0.2 μm; 2, scattering at 24.4 μm.

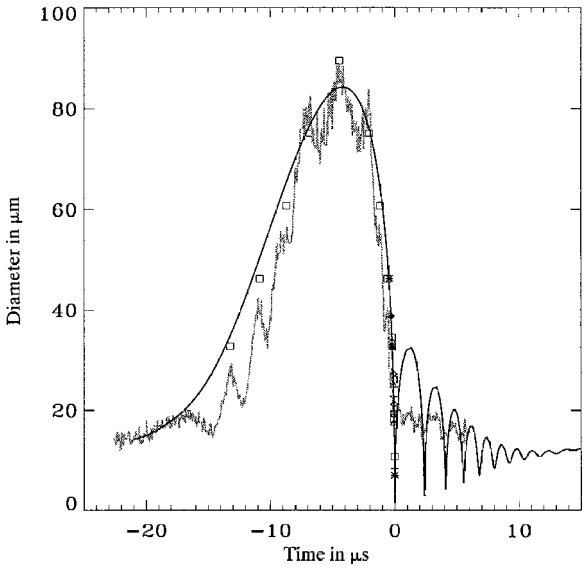

Fig. 8. Result of LC sizing (symbols) compared with hydrodynamic calculations (dark curve) and the square root of scattered intensity (light curve).

comparison with the theoretical curves. The lower traces are the inverted outputs of the SL-monitoring PMT, and the upper traces are the output of the scattered-light detectors. To improve the signal-to-noise ratio, averaging was performed for several seconds. This produced some smearing of the SL pulse as its phase drifted relative to the triggering sound field. The sudden rise in the upper traces at approximately −0.5 μs corresponds to the beginning of the laser pulse. We have synchronized the data sets by matching the time of SL, as indicated by the narrow, positive spikes in the lower traces at 0.0 μs. Careful examination of Fig. 7 reveals an unambiguous similarity—the scattering at point 1 at −0.2 μs in Fig. 7(b) corresponds to a diameter of approximately 32.5 μm in Fig. 7(a). These locations are indicated by the vertical line labeled 1. There is a similar correspondence at point 2 of 24.4 μm at −0.1 μs. When several LC peaks are moved onto one or two other peaks or minima by a change in the scattering angle, the LC can be identified unambiguously, and the size of the bubble can be determined.

Figure 8 shows the results of measurements of the diameters of several bubbles in water with the LC method. Each symbol corresponds to a different angular set of lobes or a different bubble, taken over a 3-day period. The minimum measured diameter of a bubble was 6.9 μm at 11 ns before SL. The dark curve is the result of a numerical solution to the equation for bubble motion used in Ref. 5. In the solution it is assumed that the bubble has an equilibrium diameter (i.e., the diameter in the absence of a sound field) of 14 μm and that the acoustic-pressure amplitude is 1.25 atmospheres at 26 kHz. The light curve is the square root of intensity, from which the largest diameters were deduced with the LC technique.

Figure 9 shows the last 0.5 μs before SL with the theoretical solution. Figure 10 plots the velocity from the corresponding curve in Fig. 9 to within 11 ns of SL. The bubble-wall velocity is not supersonic at this point.

Figures 9 and 10 show that the results of LC measurements are in good agreement with hydrodynamic theory. They also show the need for careful measurements near the time of SL. Theory predicts a precipitous drop in diameter within the last 5 ns or so before SL. Although it must be pointed out that the simple theory used in Figs. 9 and 10 is not valid as the velocity of the bubble-wall increases,[6] the steep slope near SL indicates that simple extrapolations to $t = 0$ may not be valid for determination of the diameter and the bubble-wall velocity at the time of SL. Also, estimates of the bubble properties at $t = 0$

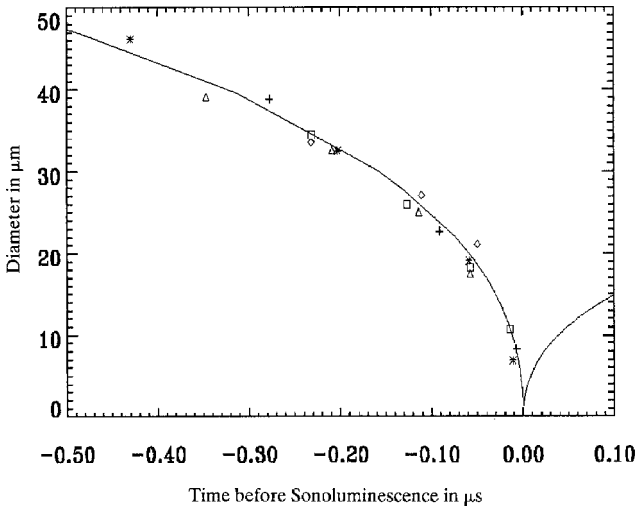

Fig. 9. Diameter near SL for several angles and bubbles over a three-day period compared with hydrodynamic calculations.

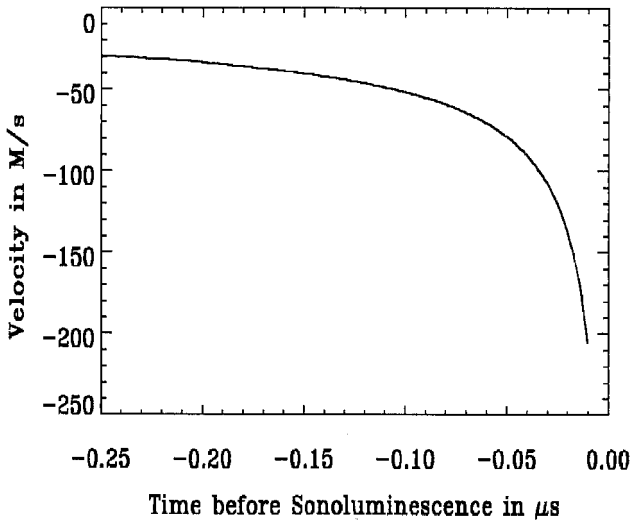

Fig. 10. Velocity near SL from the hydrodynamic calculations shown in Fig. 9.

that are based on measurements of absolute scattered intensity must take into account detector response time and changes in the bubble index of refraction.

The sizes deduced from the LC method are overlaid in Fig. 8 with the square root of the inverted PMT output that contains the lobes (light curve). The PMT output has been scaled so that it matches the peak diameter determined with the LC method. However, the data from the LC sizing do not accurately follow the square root of the PMT output, especially near SL. The discrepancy can attest to the experimental difficulties in the correct measurement of scattered intensity and to the fact that a simple diameter-squared relationship between diameter and scattered intensity is not completely accurate.

The uncertainty in measured scattering angle of ±0.25° produced a small size uncertainty that increased with increasing scattering angle and also with increasing peak number in Fig. 2. In other words, the error for each point in Fig. 2 is different. The theoretical error in the third peak at 25° might be estimated to be 0.2 μm, but the experimental errors were larger. Of much more importance is the smearing in time shown in Fig. 7. A reasonable estimate of the uncertainties can be seen from the point spread in Fig. 9, which enfolds measurement errors as well as bubble-to-bubble variations.

The largest error in sizing was the jitter of the SL relative to the sound field. In Fig. 7 the SL pulse is much wider than the 2-ns PMT limit. The time drift of the SL smeared the laser-scattering peaks, which caused uncertainties in time rather than size. This difficulty could be eliminated by triggering on the SL for laser scattering and also by triggering on the sound field to monitor stability.

Stability of the bubble and the LC scattering is essential during measurements at different scattering angles. Shifts in the driving frequency of only 0.1 Hz in 26,000 Hz can produce abrupt changes in the amplitude of the SL. With increased driving amplitude, the SL becomes brighter and more unstable. For the measurements reported here, the dimmest SL that could be detected by the RCA 5819 was used, and the phase of the SL was kept constant relative to the driving sound field during the measurements by adjustment of the driving frequency in 0.1-Hz steps. The reproducibility of the sizing data over a 3-day period indicates strong similarity between the measured bubbles.

The pulsed laser permitted viewing of the SL and the laser scattering on the same trace, as shown in Fig. 11. The time when the bubble luminesces occurs at the first minimum during the collapse phase to better than 20 ns, as determined with laser scattering. Occasional bubbles were more stable and agreed to within 2 ns, which is the limit for the PMT. The SL was never observed to occur before the first minimum in laser scattering.[5]

There are two questions that deserve some discussion. Does the bubble remain spherical, and how do the results depend on the index of refraction of the air inside the bubble, which surely must change during the cycle? To address the first question, we made some additional measurements and observations. In one set of measurements, two small PMT's were used to measure the SL simultaneously at two angles. Within the measurement accuracy for a single pulse of approximately 5%, the pulse-to-pulse energy was independent of angle and was isotropic. In another set of measurements, polarizing filters were placed in front of the PMT's. No differences could be seen, which indicated that the signal was not strongly polarized. The isotropic nature for a single pulse of light strongly suggests that the bubble is spherical during the time of SL emission. The assumption that the bubble is spherical also appears to be supported by the lack of discrepancy between the theory and the lobe measurements at multiple angles. It is difficult to imagine that patterns of LC can be moved

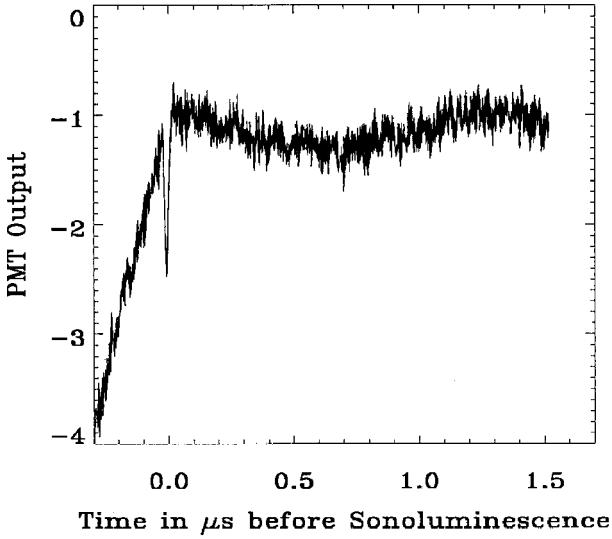

Fig. 11. Simultaneous measurement of SL and laser scattering.

relative to other patterns with matching peaks and valleys just by chance.

We are not confident that the bubble remains spherical just after SL emission. The bounces in Fig. 5 that immediately follow the compression minimum indicate that the bubble rebounds a few times after the collapse, which is theoretically predicted. On a few occasions, lobes could be seen in the bounce, and sizing was possible. In many cases, however, the scattered laser light from pulse to pulse just after SL was not nearly so repetitive as it was before SL and the bounces were not observed. It appears that the bubble is spherical during most of its cycle but may not always be spherical just after its collapse and SL emission. For that reason no sizing was attempted just after SL.

We now turn our attention to the question regarding the index of refraction of the air inside the bubble. We have assumed that the index of refraction of the air inside the bubble is 1.00. The following argument suggests that the assumption is largely valid, except near the final few nanoseconds of the collapse.

The equilibrium diameter of the bubble modeled in Fig. 8 is 14 μm. At the equilibrium diameter, the pressure and the temperature inside the bubble are equal to atmospheric pressure and room temperature, respectively. During the expansion phase of the bubble cycle, the pressure drops and the index of refraction should decrease. But the change in index cannot be large, because it cannot go any lower than 1. During the initial part of the collapse, back to the equilibrium diameter, conditions inside the bubble return to the equilibrium values. Again, the change in index is not 5significant. Hence, although the bubble is at or larger than equilibrium diameter, which covers the majority of the cycle, the index of refraction is nearly 1. The only time that the index should change significantly is during the final stages of collapse, where the diameter decreases rapidly below its equilibrium value. As can be seen from Fig. 9, these times are very short. During this stage, the pressure can reach extremely high values.[12] The index of refraction, which depends strongly on the value of equilibrium diameter, may change considerably during this phase. In fact, the entire nature of the water–air interface may change. We performed calculations for relative bubble indices of $1/1.33$ and $1.18/1.33$ to investigate the effect of a change in the index of refraction of the air in the bubble from compression near SL. The positions of the smallest LC's were relatively independent of the index change, but the scattered intensity varied by an order of magnitude. The size near SL from the LC's should, therefore, be a more accurate method of sizing the bubble than the scattered intensity.

4. Conclusions

A new laser-scattering technique has been developed to size sonoluminescing bubbles in water by the use of Mie scattering lobe clusters (LC's). More information is available from a small solid angle when the angle of scattering is varied than is available from the scattered intensity over a fixed large solid angle. The technique does not rely on an independent determination of the size of the bubble. The lobe sizing is less sensitive to changes in the bubble index than is scattered-intensity sizing. LC measurements are consistent with predictions based on simple hydrodynamic calculations and point out the importance of careful measurements near the time of SL emission.

The authors are appreciative of Tektronix for the loan of a DS602 oscilloscope and of Hamamatsu for a PMT. This work was supported in part by the Naval Postgraduate School Research Program and the Office of Naval Research.

References

1. D. F. Gaitan, L. A. Crum, C. C. Church, and R. A. Roy, "Sonoluminescence and bubble dynamics for a single, stale cavitation bubble," J. Acoust. Soc. Am. **91,** 3166–3183 (1992).
2. B. P. Barber and S. J. Putterman, "Observation of synchronous picosecond sonoluminescence," Nature (London) **352,** 318–320 (1991).
3. B. P. Barber, R. Hiller, K. Arisaka, H. Fetterman, and S. Putterman, "Resolving the picosecond characteristics of synchronous sonoluminsecence," J. Acoust. Soc. Am. **91,** 3061–3063 (1992).
4. J. T. Carlson, S. D. Lewia, A. A. Atchley, D. F. Gaitan, and X. K. Maruyama, "Spectra of picosecond sonoluminescence," presented at the 13th International Symposium in Nonlinear Acoustics, Bergen, Norway, 28–29 June 1993.
5. B. P. Barber and S. J. Putterman, "Light scattering measurements of the repetitive supersonic implosion of a sonoluminescing bubble," Phys. Rev. Lett. **69,** 3839–3842 (1992).
6. W. C. Moss, D. B. Clarke, and J. W. White, "Hydrodynamic simulations of bubble collapse and picosecond sonoluminescence," Rep. UCRL-JC-114748 (Lawrence Livermore National Laboratory, Livermore, Calif., 1993).
7. J. Schwinger, "Casimir energy for dielectrics," Proc. Natl. Acad. Sci. USA **89,** 4091–4093 (1992).
8. C. C. Wu and P. H. Roberts, "Shock-wave propagation in a sonoluminescing gas bubble," Phys. Rev. Lett. **70,** 3424–3427 (1993).
9. G. Mie, "Optics of turbid media," Ann. Phys. **25,** 377–445 (1908).
10. H. C. van de Hulst, *Light Scattering by Small Particles* (Dover, New York, 1957).
11. M. Kerker, *The Scattering of Light and Other Electromagnetic Radiation* (Academic, New York, 1969).
12. V. Kamath and A. Prosperetti, "Numerical integration methods in gas-bubble dynamics," J. Acoust. Soc. Am. **85,** 1538–1548 (1989).